Exact Derivation of the Geometric Correction Factor of the Center Notched Test Specimen, Based On Small Cracks Merging As Explanation of Softening

T. A. C. M. van der Put

Faculty of Civil Engineering and Geosciences, Timber Structures and wood technology,
TU Delft, P.O. Box 5048, 2600 GA Delft The Netherlands

ABSTRACT:
The exact derivation of the mode I geometric correction factor is given, based on the small crack merging mechanism to show that this always is the real fracture mechanism in wood. This mechanism dominates at late softening and explains fully the apparent decrease of the energy release rate of macro-crack extension as already known for mode I and is derived for mode II. The related exact theory, based on limit analysis, is discussed.

KEYWORDS: *wood, fracture mechanics, fracture kinetics, geometric correction factor of the mode I center notched test specimen, mode I and II softening behavior, mixed mode fracture criterion, oblique crack extension, small crack merging mechanism, deformation kinetics.*

I. INTRODUCTION TO SOFTENING BEHAVIOR AND CORRECTION OF THE FRACTURE ENERGY

It appears that the mechanism of small crack merging and small crack extension towards the macro-crack tip is necessary to explain total fracture behavior. It therefore is shown in Section 2 that mall crack merging towards the macro-crack tip explains fully the fracture strength of the center notch specimen, including the geometric correction factor. In Section 3, the for softening determining small crack merging mechanism is discussed and in Section 4 the necessity and form of small crack merging according to deformation kinetics theory. Determining other aspects of small crack extension are discussed in Section 5. First a correction is necessary of the fracture energy.The new, rigorous derivation of the softening behavior in [1], summarized in [2] and [3], did show that the area under the load-displacement softening curve, is not a measure of the fracture energy, but of the total external work on the specimen. The fracture energy is half this value (when linear elastic fracture mechanics is applied) and is equal to the critical strain energy release rate at the top of the loading curve. This is based on the following:

When crack extension occurs in a cantilever beam, which already is loaded by a constant load F at the free end, then the load gets an extra deflection w due to this crack extension according to Fig. 1.1.
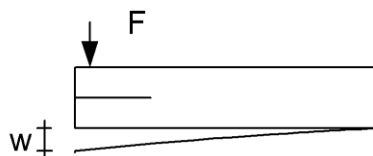

Fig. 1.1. Crack extension displacement

The total work done on the beam is $F \cdot w$ and the work for the elastic strain increase is: $F \cdot w / 2$. Thus the work, dissipated for crack extension is:

$$F \cdot w \ - \ F \cdot w / 2 \ = \ F \cdot w / 2 \ , \tag{1.1}$$

thus is equal to the elastic work of strain increase.
Therefore is the area under the load-displacement softening curve the total external work on the test specimen and is not the fracture energy alone. The fracture energy follows from half this area what is equal to the critical

strain energy release rate at the first macro-crack increment. For wood this correctly is applied for mode II,
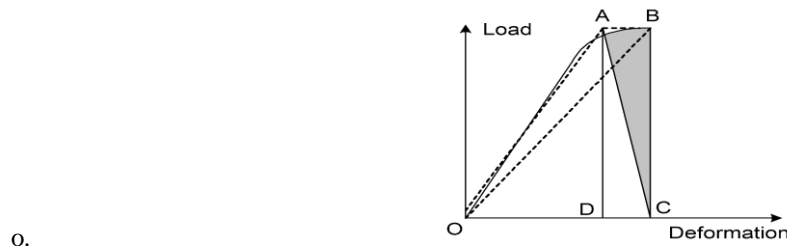

o.

Fig. 1.2. Mode II fracture energy
(see also Fig. 5.6 of [4] pg.108).

according to Fig. 1.2, where after loading to the top, the specimen is unloaded (line BO) and the elastic part of stored energy, area OBC (written as A_{OBC}) is subtracted from the total applied energy, A_{OABC}, of the loading curve, to get the right fracture energy of A_{OAB} (the area between the dashed lines as hysteresis loop). This area A_{OAB} is equal to area A_{ABC} (because triangles OAB and CAB have the same base AB and the same height BC, thus the same area). A_{ABC} is half the area of A_{ACDB}, thus half the area under the non-linear part of the loading curve. The same should apply for mode I.

For mode I however, as for other materials, wrongly the total area is regarded to be the fracture energy, thus a factor 2 too high, as shown in [1]. This is empirically verified in [5] by using the wedge-splitting test on Spruce showing the fracture energy G_f to be nearly twice as high as the energy release rate G_c in both RL and TL directions. G_f was determined from the area under the force displacement curve, while G_c (energy of incremental crack increase) followed from the finite element method. For mode I applies the following:
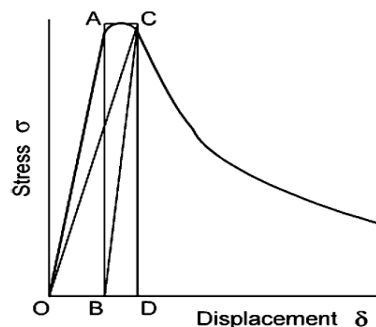

Fig 1.3. Stress- displacement of a center-notched specimen   .
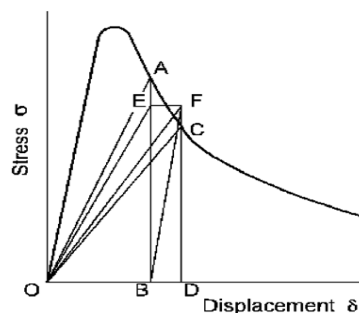

Fig 1.4. Descending branch of Fig.1.3

In the elastic-full plastic schematization of limit design is, in Fig. 1.3, the area OAB, A_{OAB}, the strain energy of a center-notched specimen, with a central crack (or with two side cracks) with a width "*b*", length "*l*" and

thickness "*t*", loaded to the stress σ. During the quasi static crack extension from B to D, in Figure 1.3, the constant external load σ does the work on the specimen of: $\sigma \cdot b \cdot t \cdot \Delta \varepsilon_{BD} \cdot l = \sigma \cdot b \cdot t \cdot \delta_{BD} = A_{ABDC}$, where $\Delta \varepsilon_{BD}$ is the strain increase due to the cracking and δ_{BD} the corresponding displacement. The strain energy after the crack extension is A_{OCD} and the strain energy increase by the crack extension thus is in Fig. 1.3: $A_{OCD} - A_{OAB} = A_{OCD} - A_{OCB} = A_{CBD} = A_{ABDC} / 2$; thus half of the external energy.

$A_{ABDC} = \sigma \cdot b \cdot t \cdot \delta_{BD} / 2$ is the amount of increase of the strain energy due to the elongation by δ , and the other half thus is the fracture energy which is equal to this increase of strain energy. The same follows at unloading at yield drop, Fig. 1.4. Because every point of the softening curve gives the Griffith strength, which decreases with increasing crack length, unloading is necessary to maintain equilibrium. The fracture with unloading step AC in Fig. 1.4 is energetic equivalent to the unloading steps AE and FC and the fracturing step EF at constant stress EB = FD = (AB + DC)/2. Thus $A_{ABDC} = A_{EBDF}$, identical to the first case of Fig. 1.3, the increase in strain energy due to crack extension is:

$A_{ODF} - A_{OBE} = A_{ODF} - A_{OBF} = A_{BFD} = 0.5 \cdot A_{EBDF} = 0.5 \cdot A_{ABDC}$, equal to half the work done by the external stresses during crack propagation and thus also equal to the other half, the work of crack extension. It thus is shown that half the area under the load-displacement curve represents the fracture energy. Thus mode I data need to be corrected while mode II data need no correction.

A further correction of the fracture energy is needed because G_f should be related, as the Griffith strength, to the effective width of the test specimen and not to the fractured ligament length because then the fracture energy depends on the choice of the initial crack length and is not comparable with G_c (which is constant). The difference between G_c and G_f has nothing to do with linear and non-linear fracture mechanics. All fracture mechanics is non-linear, but can be treated as linear full-plastic according to limit design, which is the oldest fracture mechanics analysis, and the newest in [2] by finding the solution of the Airy stress function, leading to the exact derivation of the Wu failure criterion. Thus linear elastic fracture mechanics is always applicable for wood as will be discussed later.

Regarding the fracture energy G_f a further correction is needed because there is an apparent decrease of the critical energy release rate G_c at softening. This decrease is dominant for specimens with short highly loaded fracture planes as the mode I center notched specimen. In the end stage, these planes are soon overloaded and besides macro-crack extension, small crack propagation becomes determining over the whole length of the remaining fracture plane, showing an apparent decrease of the fracture energy, when this unloading is related to macro-crack propagation alone. Thus, this strong unloading by multiple small crack extension causes a much smaller area under the unloading softening curve, than occurs at a single macro-crack extension. This diminishes strongly the mentioned factor two overestimation of the mode I fracture energy. Thus besides macro-crack extension, the clear wood strength of the fracture plane may become determining for failure in the end state. This, thus, will not occur as long as the fracture plane is not overloaded at softening as e.g. at the mode I double cantilever beam specimen, (see figures [4] pg.74 and 76) showing no apparent decrease of the fracture energy (energy release rate) during most of the softening stage of crack extension. Because step wise multiple small crack merging takes less energy than single macro-crack extension, it has to be postulated that small crack merging always takes place in the high loaded zone near the macro-crack tip and that macro-crack extension is always due to small crack extension towards the macro-crack tip. The scientific proof of this possibility is given in Section 2, by the thereupon based exact theoretical derivation of the strength of the Center Notched, test-specimen. This exact solution provides the necessary exact analytical estimation of the geometrical correction factor for this case. As known, this geometric correction factor accounts for the difference of finite specimen dimensions with respect to the same notch in an infinite plate. The properties and kinetics of small crack merging [2] are briefly discussed in Section 3 and 4. The theoretical background, necessary for understanding, is not generally known and therefore also is discussed in Section 5.

Regarding softening it has to be realized that the softening stress is a nominal stress and thus a stress far outside the fracture plane (the stress ad infinitum). Softening represents the unloading of the intact part of the specimen due to decrease of intact material in the fracture plane but also all other processes (creep, dowel failure etc.). In the fracture plane acts the constant, mean ultimate failure stress. Softening and yield drop only is possible in a constant strain rate test and is not possible in a dead load test and constant loading rate test, thus does not occur in practice.

II. DERIVATION OF THE GEOMETRIC CORRECTION FACTOR OF THE CENTER NOTCHED SPECIMEN

For comparison with other results, the mathematical flat crack (singularities) solution of the Airy stress function is chosen here for a crack in an infinite plate, which is loaded by a tensile stress σ. The stress distribution along the fracture plane, line AB of Fig. 2, then is:

$$\sigma_{Y,\infty} = \frac{\sigma}{\sqrt{1-(a/x)^2}} \qquad x > a \tag{2.1}$$

where $2a$ is the crack length and x is the distance from the center of the crack. This stress distribution is according to the solution of the Airy stress function of [6]. Such a solution satisfies the equilibrium, compatibility and boundary conditions and thus is an exact solution.

To obtain the ultimate state of the specimen given in Fig. 1, we may cut out the specimen dimensions from the infinite plate, as is given in Fig. 2. Next we may multiply the stress $\sigma_{y,\infty}$ by a (by definition stress independent) factor Y with such magnitude that the resultant shear loading $2R$ in the planes AD and BC of Fig. 2 becomes zero. There remains an equilibrium system in those vertical planes giving an internal equilibrium system in the cut-out specimen which, as such, has no influence on the ultimate state. It, of course, is possible to superpose a neutralizing equilibrium system providing stress free vertical planes. As condition for zero values of R, the sum of the normal stresses in the upper plane AB should be equal and opposite to the normal stresses in the bottom plane CD. Thus the total sum of the (vertical) normal stresses on the cut out specimen should be zero giving:

$$\sigma W = 2 \int_a^{W/2} \sigma_y dx = 2 \int_a^{W/2} \left(Y\sigma / \sqrt{1-(a/x)^2} \right) dx = Y\sigma W \sqrt{\left(1-(2a/W)^2\right)}, \tag{2.2}$$

and the stress multiplication factor thus is:

$$Y = 1/\sqrt{1-(2a/W)^2}. \tag{2.3}$$

The stress intensity factor K_I due to the critical small crack concentration follows from:

$$K_I = \sigma_y \sqrt{\pi a_c} = \sigma_y \sqrt{\pi 2(x-a)} = \left(Y\sigma / \sqrt{1-(a/x)^2} \right) \sqrt{\pi 2(x-a)} = Yx\sigma \sqrt{2\pi/(x+a)} \tag{2.4}$$

As shown in [2], the small crack merging towards the macro-crack tip causes the macro-crack extension. Whenthe nearest, determining small crack tip is situated at a distance x, then the one sided small crack merging distance to the macro-crack tip is $x-a$, which is equal to half the small crack length c of row A of Section 3. Thus: $c = (x-a)$, and total $2(x-a)$ applies, of both sides of two sided macro-crack extension of the initial crack length of $2a$. This also applies when the macro crack-tip has become sharp enough to takes part in the crack merging process. Then all active crack tips extend over a distance c, which is equal to $c = (x-a)$ in the analysis. For $x \to a$, the lowest, thus first occurring, initial flow value for K_I of eq.(2.4), becomes:
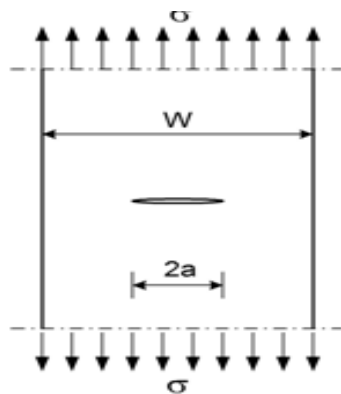
$$K_I = Y\sigma\sqrt{\pi a} \tag{2.5}$$
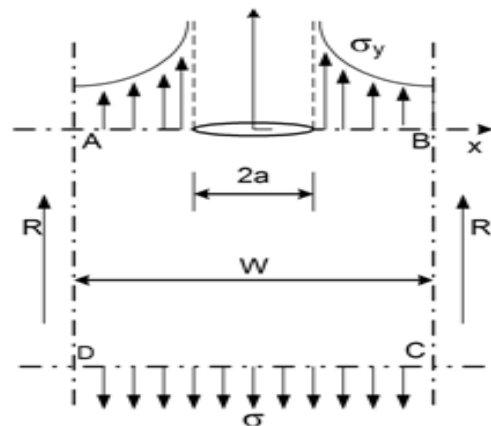

Fig. 1. CN test specimen

Fig. 2. Cut out of the specimen from the infinite plate

This is identical to the results of other methods, showing the mathematical flat crack, singularity solution, to apply for the smallest initial small crack system and to represent an estimate of the start of crack extension. For initial small cracks smaller than c_c of eq.(3.2), instable crack propagation occurs to a new equilibrium crack-length, which is on the Griffith locus, eq.(3.1). When different small crack-lengths are supposed to act, a mean value factor c_1 has to be inserted for a mean length value. Then the geometric correction factor with respect to the stress in the infinite plate is: $Y\sqrt{c_1}$. But, by comparing this result with other exact geometric correction factors, given in [7], the value $c_1 = 1$ is found. Thus the derived geometric correction factor Y is comparable to the other solutions of Tada, Feddersen, Koiter, Isida and Irwin. The value $c_1 = 1$ thus means that the first small crack merging process, row A of Section 3, solely act at the start of further crack extension, as predicted by theory.

The value Y, according to eq.(3): $Y = 1/\sqrt{1 - (2a/W)^2}$, can be seen as a mean value, intermediate between the, in [7] given, values of Koiter et al. and Feddersen around $Y = \sqrt{\sec(\pi a/W)}$ and the solution of Irwin: $\sqrt{(W/\pi a)\cdot\tan(\pi a/W)}$.

In Table 1, eq.(3) is compared with the solution of Irwin and the usual applied Feddersen equation.

The precise description by the exact derivation shows that small crack merging does not only explains softening but is the basic mechanism of all crack extension. This will be discussed further in Section 3. The possibilities of the singularity approach are very limited. For instance extension of the theory for crack bridging with a plastic zone of length $a_0 - a$ at the initial crack tip of the elongated crack length a_0, changes eq.(2) to:

$$\sigma W - 2\sigma_t(a_0 - a) = 2\int_{a_9}^{W/2} \sigma_y dx = 2\int_{a_0}^{W/2}\left(Y\sigma/\sqrt{1 - (a_0/x)^2}\right)dx = Y\sigma W\sqrt{\left(1 - (2a_0/W)^2\right)} \qquad (2.6)$$

where σ_t is the ultimate (plastic) tensile stress of the bridging area. The stress multiplication factor then is:

$$Y = \left(1 - 2(\sigma_t/\sigma)(a_0 - a)/W\right)/\sqrt{1 - (2a_0/W)^2} \qquad (2.7)$$

Table 1. Comparison of linear elastic Geometric correction factors

$2a/W$	$Y = \sqrt{\sec(\pi a/W)}$	$Y = 1/\sqrt{1 - (2a/W)^2}$	$\sqrt{(W/\pi a)\cdot\tan(\pi a/W)}$
0.1	1.006	1.005	1.004
0.2	1.025	1.021	1.016
0.3	1.059	1.048	1.040
0.4	1.112	1.091	1.075
0.5	1.189	1.155	1.128
0.6	1.304	1.250	1.208
0.8	1.799	1.667	1.565
0.9	2.528	2.294	2.113
0.95	3.570	3.203	2.918
	Feddersen	Eq.(3), crack merging	Irwin

showing this factor to be stress dependent and thus showing that by maintaining a singularity, the approach is not applicable for theory extensions. The general accepted replacement of surface energy by strain energy release rate, which is equal to bond-breaking and plastic dissipated energy (while maintaining the old stress independent geometric correction factor) thus is not exact. New exact theory extensions (necessary e.g. for combined loading) only may follow from limit analysis [2] what will be discussed in Section 5. First the basic crack merging mechanism has to be discussed.

III.   SOFTENING BY A CRACK MERGING MECHANISM
3.1. Mode I tension tests
For a full description of softening, at crack extension of a test specimen, the damage theory of Deformation Kinetics [8], also has to be applied at measuring compliance changes. This theory is discussed here in Section 4. A fundamental derivation of softening behavior, at standard climatic conditions, is also possible by the energy

method of the Griffith theory. This is developed and discussed in [1] and [2], Chapter 3, and is the basis for understanding the following. For a not limiting, sufficient long fracture plane of the test specimen, G_c, the critical energy release rate, is constant at every point of the softening curve and therefore the Griffith locus, eq.(3.1), (which is eq.(3.12) of [2]), applies:

$$\varepsilon_g = \sigma_g / E + 2 G_c^2 E / \pi \sigma_g^3 b l \tag{3.1}$$

The top of this curve has a vertical tangent $d\varepsilon_g / d\sigma_g = 0$, occurring at a crack length of:

$$c_c = \sqrt{W l / 6\pi} . \tag{3.2}$$

where $l \geq \square \, 4a$ is the length, or the working length (a St. Venant's distance), of the test specimen. For a distribution of small cracks, W and l in eq.(3.2) are the st. Venant crack distances as critical small crack distances. This critical initial distance, of about 2 to 2.2 times the crack length, is predicted by Molecular Deformation Kinetics theory [8] and applies for the strength of all solids according to the mechanism of Fig.3. When the remaining fracture plane is too short, it becomes overloaded at macro-crack extension causing unloading by small crack extension everywhere in the remaining fracture plane also outside the crack tip region. At that point there is not enough strain energy any more for single macro-crack extension and unloading takes place by small crack merging while the macro-crack extends by small-crack propagation towards the macro-crack-tip. The departure of the softening behavior from the Griffith locus, by the gradual decrease of G_c, thus is due to clear-wood failure of the high loaded fracture plane, which takes less energy for propagation to small-crack rows B and C of Fig. 3, than for a single macro-crack extension. This clear wood fracture plane is equally strong everywhere and thus contains a critical small crack density over the whole fracture plane at the start of small-crack softening. At this critical small-crack density, the crack distance is about equal to the crack length, as given by row A below.
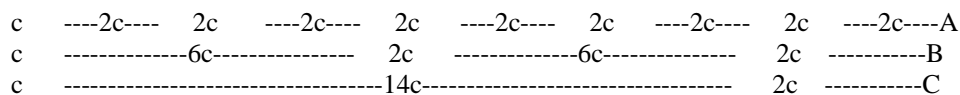
```
c    ----2c----    2c    ----2c----    2c    ----2c----    2c    ----2c----    2c    ----2c----A
c    --------------6c----------------    2c    --------------6c---------------    2c    ----------B
c    ------------------------------------14c----------------------------------    2c    ----------C
```

Fig. 3. Crack rows of successive processes.

When 2 cracks of A merge, a crack length of 6c occurs, given by row B which is the site for the next merging reaction, giving a crack length of 14c, as shown by row C. The area of the intact fracture plane of row A then is twice the intact area of row B and four times the area of row C. Because this system of crack merging takes less energy at lower stresses than macro-crack propagation by one macro-crack alone, it provides a more probable solution.

As shown in chapter 3 of [2], the decrease of the Griffith values σ_g and G_c, then is fully explained by the strength of the intact part of the fracture plane, which remains at the ultimate state $\sigma_g = \sigma_m$, as is verified by the measurements, eq.(3.1), in the form of eq.(3.19) of [2], of the softening curve, is according the measurement of [9] by Figure 3.6 and 3.7 of [2] and precisely explains the decrease of σ_c, the top-value of the softening curve,

The in [2] and [4] discussed small crack mode I behavior, predicts analogues behavior for mode II. This is discussed in the next Section 3.2.

3.2. Mode II shear tests

In Yoshihara [10], [11], results of mode II tests, called asymmetric four point bending (AFPB) tests, are given applied on very long sub-critical initial crack lengths, which clearly represent the softening stage at loading, because the measured K_{IIc}-values were a factor 3 to 4 lower than those of the control tests on standard end-notched flexure (ENF) test-specimens. Of standard equation for this case, eq.(3.3), the chosen value of a and measured strength value τ_0 are known and K_{IIc} is determined by measuring the energy release rate G_{II} by the compliance method at different crack lengths and, as control, by the finite element virtual crack closure method.

$$K_{IIc} = \tau_0 \sqrt{\pi a} \cdot Y\left(a / W\right) \tag{3.3}$$

The geometric correction factor $Y\left(a / W\right)$ is deliberately not determined theoretically, but is simply found as

equating value: $Y\,(a\,/\,W\,) \equiv K_{IIc}\,/\,(\tau_0\sqrt{\pi\,a}\,)$ (3.4)

There thus is no control on applying right parameter values and it is e.g. not noticed that a wrong, not measured, stiffness factor is used. However, this factor is the same for all cases and has no influence on the in the following presented relative values and on the control of the crack merging theory:

The data of Yoshihara [10], [11] are purely empirical, based on measurements and empirical methods as the compliance measurement and finite element calculation. Therefore it is empirically shown, that the real mean shear strength on the intact part of the fracture plane is determining and not the measured apparent K_{IIc} - value, which is too low for macro-crack extension. For macro-crack extension applies that according to eq.(1) of [10], for the top of the loading curve, at $a\,/\,W\,=\,0.7$:

$$K_{II,0}\,=\,\frac{3\,P}{4\,B\,W}\sqrt{\pi\,a_c}\,=\,\tau_n\sqrt{\pi\,a_c}$$ (3.5)

because then $f\,(a\,/\,W\,)\,=\,1$ and the nominal Griffith shear stress is: $\tau_n\,=\,3\,P\,/\,4\,B\,W$ (3.6)

As follows from [2], eq.(3.13) is the critical crack length: $a_c\,=\,\sqrt{b\,l\,/\,6\,\pi}$ for mode I, according to Fig. 3.1. For the AFPB-test is, $b\,=\,W$ and $l\,=\,c_1 W$, proportional to *W,* as a Saint-Venant distance. A similar relation applies for mode II, following from the Griffith locus derivation for compression and shear. Thus

$$a_c\,=\,\sqrt{W\,c_1 W\,/\,6\,\pi}\,=\,c_2 W$$ (3.7)

For higher values of *a,* when $a\,/\,W\,>\,0.7$ is, as applied in Yoshihara [10], [11]:

$$K_{II}\,=\,\tau_n\sqrt{\pi\,a}\,\cdot\,f\,(a\,/\,W\,)$$ (3.8)

It is shown in [2], Section 3.6, that at a far stage of softening, the small crack merging mechanism shows that at any moment the strength of the intact fracture area is determining for the strength. This can be interpreted that not the nominal stress but the ultimate real stress f_u in the fracture plane is determining. Thus eq.(3.5) becomes:

$$f_u\,=\,K_{II,0}\,/\,(\sqrt{\pi\,a_c}\,\cdot\,(1\,-\,a_c\,/\,W\,))\,=\,K_{II,0}\,/\,(\sqrt{\pi\,c_2 W}\,\cdot\,(1\,-\,c_2\,))$$ (3.9)

and eq.(3.8): $f_u\,=\,K_{II}\,/\,(\sqrt{\pi\,a}\,\cdot\,(1\,-\,a\,/\,W\,)\,\cdot\,f\,(a\,/\,W\,))$ (3.10)

and from eq.(3.9) and (3.10) follows:

$$\frac{K_{II}}{\sqrt{\pi\,a}\,\cdot\,(1\,-\,a\,/\,W\,)\,\cdot\,f\,(a\,/\,W\,)}\,=\,\frac{K_{II0}}{\sqrt{\pi\,c_2 W}\,\cdot\,(1\,-\,c_2\,)}\quad \text{or:}$$

$$\frac{K_{II}}{\sqrt{a\,/\,W}\,\cdot\,(1\,-\,a\,/\,W\,)\,\cdot\,f\,(a\,/\,W\,)}\,=\,\frac{K_{II0}}{\sqrt{c_2}\,\cdot\,(1\,-\,c_2\,)}\,=\,c_4\quad\text{(constant)}$$ (3.11)

According to Fig.12 of Yoshihara [11], there is no difference (by volume effect) between the data for W = 40 mm and W = 20 mm, thus mean values of both can be regarded.

For *a/W* = 0.7, $K_{II}\,=\,0.79$ MPa$\sqrt{m}$ thus: $c_4\,=\,3.15$ (3.12)

For *a/W* = 0.8, $K_{II}\,=\,0.71$ MPa$\sqrt{m}$ thus: $c_4\,=\,3.3$ (3.13)

For *a/W* = 0.9, $K_{II}\,=\,0.52$ MPa$\sqrt{m}$ thus: $c_4\,=\,3.28$ (3.14)

$f\,(a\,/\,W\,)\,=\,1.0$ for *a/W* = 0.7 and is 1.2 for *a/W* = 0.8 and is 1.67 for *a/W* = 0.9

Thus the mean value of c_4 is: $c_4\,=\,3.24$ Numerically this calculation is:

$0.79/(\sqrt{0.7}\,(0.3)\cdot 1)\,=\,3.15$ and: $0.71/(\sqrt{0.8}\,(0.2)\cdot 1.2)\,=\,3.31$ and: $0.52/(\sqrt{0.9}\,(0.1)\cdot 1.67)\,=\,3.28$

It thus is confirmed by the data of Yoshihara [10], [11], that the real mean shear strength of the intact part of the fracture plane is determining and determines the occurring apparent K_{II} - value, which is too low for real macro-crack extension. It thus is shown that, also for mode II, small crack merging and extension towards the macro-crack tip is determining for fracture.

IV. DEFORMATION KINETICS BEHAVIOR

4.1. Basic properties of some relevant processes in wood

As known, strength and time dependent behavior of materials only can be explained by the physical and chemical processes of bond breaking and bond reformation and thus by statistical mechanics and reaction kinetics. In the format of limit analysis, of the in [8] developed equilibrium theory of deformation kinetics, aspects as creep, damage, aging, annealing, nucleation (see [12]), transformations, as glass transition (see [13]), rubber behavior, diffusion, etc. are all explained by the same constitutive equation. The consequence is that the absurd, contradictory phenomenological models, as the free volume model for glass-transition, the instability model of nucleation and the extrapolated flexible chain model, with non-existent linear viscoelastic relaxation spectra for rubber behavior and creep of materials, etc., are rejected and excluded.

Thus as consequence, time dependent behavior of wood, timber and notched wood is non-linear and the processes follow the molecular deformation kinetics equations with a correlation close to one, only determined by the measuring precision of the testing equipment, showing the molecular large number statistics. The variability occurs among different wood specimens of the series. Every piece of wood thus is significantly different of each other and thus is an unique giant molecule. The parameters, as concentration, activation energy and volume, of the processes can e.g. be found by creep, relaxation, recovery, long duration and complex loading-history tests at different temperatures, loading rates and moisture contents, measuring response and hysteresis and decrease of the modulus of elasticity, etc.

Regarding fracture, creep tests of wood, at normal test conditions, may show a quick fracture process at the start of loading as follows from the high enthalpy, which is high enough for primary C-O-bond or C-C-bond rupture. The fact that this process is quick, despite the high activation energy, shows that the internal stress is high, as occurs at initial crack extension at imperfections to a stable length and stable direction, providing then the sites for following extensions. However, the concentration of sites is very low and this primary bond breaking process thus is of minor importance in the ramp loading tests of fracture mechanics. Comparable (high enthalpy) processes only dominate at a high stress level e.g. in controlled crack growth tests. Dominating during ramp loading are the viscoelastic and plastic processes. The coupled processes according to Fig. 3 are confirmed to act in [8]. The main process (of side group readjustment and failure by cooperative hydrogen bond breaking) is coupled to a process with a long delay time (and a very low initial flow unit density), which shows irreversible strain at an activation energy which is high enough for primary bond breaking (see e.g. Fig 5.10 of [8]). This second process can be regarded to start at an ultimate strain of the first process. Regarding the response, these coupled processes show each a constant activation volume parameter, independent of initial stress and temperature and thus show, outer the time-temperature equivalence, also a time stress equivalence, what means that the relaxation time decreases with increasing stress and increases with decreasing stress, what explains in the last case, the quasi permanent deformation of wood at unloading, which only can be recovered by heating and moistening. The consequence of the decreasing relaxation time with stress increase is that the primary bond-breaking process, thus fracture, only is noticeable, within the time-scale of ramp-loading, close to the top of the loading curve. This means that the lower bend off of the loading curve is not due to fracture, and therefore is not correlated to fracture (as also found empirically).

4.2. Deformation kinetics behavior of crack merging

The crack-merging analysis of Section 3, shows that in general:

$2c_{n+1} = 2 \cdot 2c_n + 2c_0$, giving $2c_1 = 6c_0$ and $2c_2 = 2 \cdot 2c_1 + 2c_0 = 14c_0$.

The increase of the crack length is: $\Delta(2c)' = 2c_{n+1} - 2c_n = 2c_n + 2c_0$.

Including the initial crack length of $2c_0$, the increase of the total crack length is:

$$\Delta(2c) = 2c_{n+1} - 2c_n - 2c_0 = 2c_n \tag{4.1}$$

More general for all merging cracks during time Δt this is:

$$\Delta(c) = \beta_1 \cdot c \cdot \Delta t \tag{4.2}$$

and as a damage deformation kinetics equation this is:

$$dc / dt = \beta_2 \cdot c_0 \cdot \exp(\sigma\varphi) \tag{4.3}$$

when the initial site concentration c_0 is high as applies for row A of Fig. 3..

Because the decrease of the energy release rate (fracture energy) is proportional to the area decrease of the fracture plane area due to the small cracks extension, eq.(4.1) also may become:

$$\Delta(2c)/(2c) = -\beta_2 \cdot \Delta(G_c) \tag{4.4}$$

when the initial concentration c is low as e.g. applies for row B of Fig. 3 where the concentration of sites c is identical to the product of the reaction of row A. Eq.(4.4) can be expressed in mean crack velocities by replacing c by $\dot{c} \cdot t$, with $\dot{c}$ as mean crack velocity. Thus: $\Delta(2c)/(2c) = \Delta(\dot{c}t)/\dot{c}t = \Delta\dot{c}/\dot{c}$. Then integration of eq.(4.4), leads to:

$$G_{c,a} = G_{c,a,1} - \gamma \cdot \ln(\dot{c}), \tag{4.5}$$

This is measured in [14] and mentioned in [15] for the irreversible work of loading cycles. However, the kinetics, of the data of [14], shows the reaction to be a mechanosorptive effect and thus only may occur in this form when moisture movement is possible during the test.

Row A of Fig. 3, determines the clear wood strength which shows, by the property, that the stress intensity factor can be regarded as material property, that always the same small cracks with the same crack-tip radius r_0 are acting everywhere and therefore the common engineering strength applies. Thus, because $r_0/c = r_0/c_0$ is always the same, is:

$$K_I/K_{Ic} = (\sigma_y\sqrt{\pi c_0})/(\sigma_t\sqrt{2\pi r_0}/2) = \sigma_y/\sigma_t\sqrt{r_0/2c_0} = \sigma_y/f_t, \tag{4.6}$$

and is the strength proportional to K_{Ic} and thus eq.(4.3) can be written:

$$\frac{\sigma_t}{f_t} = 1 + \frac{1}{n}\ln(\frac{\dot{c}}{\dot{c}_m}) = \frac{K_I}{K_{I,m}} \tag{4.7}$$

This semi log-plot, eq.(3.28) of [2], is given, as empirical line, in many publications, based on data of e.g. ceramics, polymers, metals and glasses and is e.g. given in [15] for wood. Eq.(4.7) shows that now G_c, as well the elasticity modulus E, are proportional to the strength.

The kinetics shows the same behavior for the macro notch as for clear wood, indicating that small-crack propagation is always determining. As shown in [8], two coupled processes act initially, showing the same time-temperature and time-stress equivalence. One process, with a very high density of sites, provides the sites of the second low site density process, as follows from a very long delay time of the second process. The notched specimen discussed here also shows the low concentration reaction, which is indicated by the strong softening behavior at ramp loading. Here the macro crack extension acts as the second low (crack-) concentration process coupled to the small crack merging process. This failure mechanism thus applies for every bond breaking process at any level.

V. RELATED BASIC THEORY

5.1 Introduction

The now accepted singularity approach does not say anything about the local fracture mechanism. Of course the singularity with the infinite stress at a zero crack length does not exist. The center of the singularity is an open space. For predicting reliability and to give a physical meaning, it is necessary to leave the non-existent singularity approach, which in fact prevents a real description of the ultimate state. Removing the singularity always leads to new theory (see e.g. [16]). Removing the singularity concept for black holes in Astronomy, provided many important new theories where thousands of scientist are working on. Leaving the singularity approach in fracture mechanics, necessary for description of real behavior [1-3], thus should at least lead to studying the possibilities and joining the new age, instead of leading to ignorant rejection. Necessary thus is the exact approach. Exact theory represents the law of nature, which prescribes and determines behavior. It provides the only way of prediction and explanation of behavior and thus of test results and provides the only way to real calculable reliability. It therefore has to be shown that new theory is related to all other exact theory in that field as given by e.g. [1–3] and other referenced literature. Wood has to be regarded as a reinforced isotropic material. The existence of an isotropic matrix in wood follows not only from material analysis, but also from the high compression strength at confined dilation with the absence of failure by triaxial hydrostatic compression, (what is not the case for anisotropy, because for equal triaxial stresses, the strains then are not equal and yield remains possible). Because of this, the, in [17] derived orthotropic critical distortional energy principle applies for initial yield. Perpendicular to the grain, isotropic behavior of the wood matrix is e.g. shown by oblique grain tests (see [19]) which show hardening, after orthotropic flow, leading at a later stage to equal ultimate stresses, independent of orientation.

The failure criterion of clear wood and of timber ([17], [19], [20]) and the failure criterion by a single notch ([2]), is the same, showing that small-crack extension towards the macro-crack tip is the cause of macro-crack extension. This is confirmed by the fact that the stress intensity factor is the same independent on the macro-form and dimensions of the notch. It also is confirmed by molecular deformation kinetics, showing the same processes in clear- and in notched wood. Also the exact solutions given in this article of the geometric correction factor and of the strength behavior of long post-critical crack lengths is totally based on small crack behavior. The small-crack merging mechanism explains [2] precisely the mode I softening curves of [9]. The failure criterion [17] shows no coupling term between the normal stresses at "flow", and thus shows no dowel action of the reinforcements and there only is a direct interaction of the reinforcement with the matrix and the matrix stresses determine the stresses in the reinforcements. Because the initial small cracks in wood are in the matrix and start to extend in the matrix, the stress equilibrium condition of the matrix by the matrix-stresses has to be regarded. Because this failure of the matrix, the isotropic solution of the matrix stresses also has to be regarded in the end state. The total stresses, due to the reinforcement then follow by multiplication of the modulus of elasticity ratio.

5.2. Limit analysis theory

The blunting at the top of the loading curve of test specimens, visible when the testing rig is stiff enough to allow the test to follow the theoretical softening curve, shows that there is a plastic range, which is extended enough to make any stress redistribution possible. This means that limit analysis has to be applied for the ultimate strength analysis providing always possible exact solutions. This analysis (also followed by Griffith), is based on an elastic-full plastic schematization of the loading curve. This means that in stress space, the flow criterion is a single curve and for "plastic" dissipation, the stress vector should be along (tangential to) the concave curve, and the strain vector should be perpendicular to the stress (normality rule) what means that the (maximum) extremum variational principle applies for "flow" and thus the virtual work equations apply and thus the theorems of limit analysis with the lower and upper bound solutions exist for any allowable equilibrium system, following as solution of the Airy-Stress function. Fracture of wood thus is a common boundary value problem of the strength at the crack boundary. This is derived in van der Put [2] Chapter 2, and it appears that, for any load combination, fracture occurs by reaching the uniaxial tensile strength at the crack boundary near the crack tip. This uniaxial tensile stress is a measure of the cohesion strength and leads to the mixed mode Wu-equation:

$$K_I / K_{Ic} + \left(K_{II} / KI_{IIc} \right)^2 = 1 \qquad (5.1)$$

as exact solution [2], as well of the isotropic Airy stress function of the matrix stresses, as of the orthotropic Airy stress function of the total stresses. Only for mode I the crack extension is collinear. For shear (mode II) loading and for combined mode I and II loading, oblique crack extension occurs.
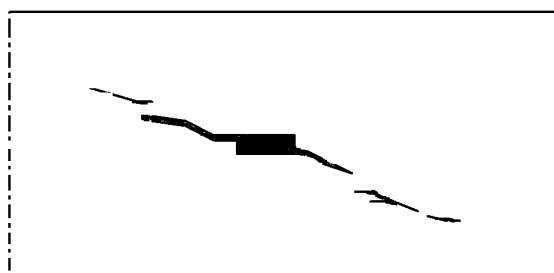

Fig. 4 - Shear failure by the asymmetric four point bending
test with small center-slit. Sketch after the photo of [21]

An example of oblique crack extension according to theory is given in Fig. 4, of mode II failure of, perfect defect free, small clear specimens of air-dry Agathis wood at normal climate conditions. This behavior according to theory is possible because of the absence of interference with a small cracks system. Normally there always is a pronounced initial small crack system as e.g. measured by Wu [22] were by interference, "bridged" oblique small crack extension occurs as given by Fig. 5.
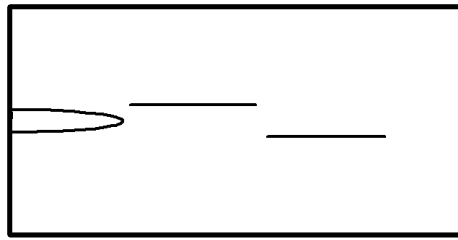
Fig. 5. Schematic crack extension by
"skipping across fibers" of Wu [22]

Although the ultimate shear stress occurs at the crack tip, there is no shear failure at mode II loading, and thus no collinear crack propagation, but always tensile failure as explained e.g. in [23], Section 4, given analysis of the end-notched flexure test, showing that plastic deformation is necessary for stress redistribution to make collinear "mode II" (tensile) splitting possible and thus not fits in the linear elastic approach.Collinear crack extension is possible by interference of tensile stresses, causing tensile failure in the weakest plane (along the grain) as is given by Fig. 6 by small crack merging, where each crack is propagating in the two directions towards each other.
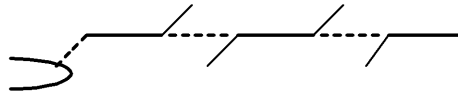

Fig. 6. Collinear small crack merging.

As mentioned, failure of the matrix is determining for the start of failure. This follows e.g. for Balsa wood, which is highly orthotropic, but shows the isotropic failure ratio of $K_{IIc} / K_{Ic} \approx 2$ of the isotropic matrix material. Also the oblique crack extension of strong wood with a high reinforcement content, according to Fig. 4, shows the isotropic oblique angle at the start of crack extension, showing the matrix to be determining for initial failure.It is therefore a requirement for an exact orthotropic solution, applicable to wood, to satisfy the equilibrium condition for both, the total stresses as well as the matrix-stresses. The general accepted and applied mathematical flat crack solutions of the Airy stress function (singularity approach), can be modified to represent a failure criterion at the crack-tip boundary r_0 by inserting $r = r_0$ in the equations instead of letting $r \to 0$. This can be used to obtain lower bound collinear single mode solutions.A right mixed mode failure criterion is however not possible. Mostly a linear relation between stresses, is given which therefore does not apply for wood because the parabolic Wu-equation is the exact solution [2] verified by measurements [22]. This also was verified e.g. by the tests of [24] done at the TL-system on eastern red spruce at normal climate conditions using different kinds of test specimens. The usual finite element calculations provided the geometric correction factors, and the stress intensity factors K_I and a lack of fit test was performed on the data, at the for wood usual variability, assuming five different failure equations. Statistical lack of fit values are tabulated in Table 2 of [24] and as can be seen from that table, the one failure criterion that cannot be rejected due to lack of fit is the by Wu proposed equation, eq.(5.1), which also is shown to fit clear wood [19] and is derived exactly.

Table 2. Lack of fit values for different failure criteria [24]

Failure criterion	p value
$K_I / K_{Ic} = 1$	0.0001
$K_I / K_{Ic} + K_{II} / K_{IIc} = 1$	0.0001
$K_I / K_{Ic} + \left(K_{II} / K_{IIc} \right)^2 = 1$	0.5629
$\left(K_I / K_{Ic} \right)^2 + K_{II} / K_{IIc} = 1$	0.0784
$\left(K_I / K_{Ic} \right)^2 + \left(K_{II} / K_{IIc} \right)^2 = 1$	0.0001

and the Wu-equation, eq.(5.1), thus is no longer an arbitrary empirical equation, but is the highest lower bound solution which is equal to the real solution. The by the theory predicted oblique crack extension and interference with approaching small cracks, causes the by Wu, [22], measured displacement of the crack boundary and the skipping over fibers, given in Fig.5 and 6.

VI. CONCLUSIONS

- An exact explanation is given of the apparent decrease of the (macro crack) stress intensity factor. This appears to be caused by a small crack merging mechanism, which takes less energy than a single macro-crack extension. The data of [10], [11] on long over-critical initial crack lengths, follow the theory precisely. It is probable that this small crack merging mechanism determines always the strength of timber.
- The properties following from exact strength theory of wood should be accounted in a right fracture mechanics theory. It therefore is necessary to regard:
- that limit analysis applies, with elastic-full plastic behavior and thus elastic up to fracture,
- that wood behaves as a reinforced material, and the solutions of the isotropic Airy stress function of the matrix stresses as well as the orthotropic Airy stress function are needed,
- that reaction kinetics and the general applicable failure criterion indicate that, small-crack processes are always determining for fracture.
- that for overloaded fracture planes of long post-critical initial cracks, the strength of the intact part of the fracture plane determines softening by the maximal possible loading state. The intact area is determined by the small crack merging mechanism which e.g. explains the factor 2.5 to 3.9 too low stress intensity factors of [10], [11].
- The theory predicts that for mode II and for combined loading, the right fracture energy is found by the finite element virtual crack closure technique applied on oblique crack extension in the right direction. This is verified for clear wood and is not the case for an assumed collinear crack.
- There is no difference between linear elastic- and non-linear fracture mechanics because for both approaches linear elastic behavior is regarded up to failure and plastic flow. This is possible because by the virtual work approach at the ultimate state there is no influence on the strength of the loading path followed and of initial stresses and internal equilibrium systems. The critical energy release rate is in both cases determined by plastic behavior. In fact always the linear – full plastic approach of limit analysis applies for the boundary value approach and ultimate state at the crack-tip boundary.
- The start of softening by small crack extension can be given by a critical macro-crack length for the space were the critical small crack density occurs. Further empirical investigation is necessary to find which processes act together providing the constants.
- Because the macro-crack kinetics is the same as for clear wood, this small-crack behavior is always determining (see last part of Section3.6 of [2]).
- For too long initial cracks as in [11], the strength of the intact part of the fracture plane is always determining and explains the measured too low stress intensity.
- Small-crack merging explains precisely the softening curve (of [9]) by the strength (or plastic flow stress) of the intact part of the fracture plane, which is always in the ultimate state and is most probable because it requires less energy than single macro-crack propagation ([2], Section3.5 and 3.6) and shows in rate form the necessary molecular deformation kinetics equation of this damage process. (see [8]).
- Because at the crack boundary, or at the elastic-plastic boundary at the crack-tip, the elastic solution as well as the ultimate strength solution applies, according to limit analysis, it is necessary to solve the elastic solution of the isotropic matrix stresses and then calculate the stresses in the reinforcement in proportion to the modulus of elasticity of matrix and reinforcement. This way of calculation is necessary for wood because of the single, direct interaction of the reinforcement and matrix and the start of crack extension in the matrix.

REFERENCES

[1]   van der Put T.A.C.M., Softening behavior and correction of the fracture energy. Theoretical and Applied Fracture Mechanics vol. 48 issue 2 October, 2007. p. 127-139.
[2]   van der Put T.A.C.M., A new fracture mechanics theory of wood", Nova Science Publishers, New York, 2011.
[3]   van der Put T.A.C.M., Advances in Mechanical Engineering Research, Vol. 2. Chapter 1: Fracture Mechanics of Wood and Wood like reinforced Polymers, Nova Science Publishers, INc. New York, 2011
[4]   Smith I., Landis E, Gong M, Fracture and Fatigue in Wood, John Wiley, Chichester, England, 2003
[5]   Vasic S., Smith I, and Landis E (2002) "Fracture zone characterization-micro-mechanical study", Wood and Fiber Science, 34 (1): 42-56. (Vasic et al. (2002),)
[6]   Westergaard H.M., Trans. ASME, J. Appl. Mech. Vol. 61, 1939, pp A49 – A53.
[7]   Tada H., Paris .P.C. and Irwin G,R. The stress analysis of Cracks Handbook". Del Research Corporation, St. Louis, Missouri, 1985, H. Tada, Paris and G.R. Irwin.

[8]   van der Put T.A.C.M., Deformation and damage processes in wood, Delft University Press, The Netherlands, (1989).
[9]   Boström ., Method for determination of the softening behavior of wood etc. Thesis, Report TVBM-1012, Lund, Sweden, (1992).
[10]   Yoshihara, H. (2012) Mode II critical stress intensity factor of wood measured by the asymmetric four-point bending test of single-edge-notched specimen while considering an additional crack length, Holzforschung, 66, pp 989-992.
[11]   Yoshihara H. (2008) Mode II fracture mechanics properties of wood measured by the asymmetric four-point bending test using a single-edge-notched specimen, Eng. Frac. Mech. 75 pp.4727-4739.
[12]   van der Put T.A.C.M. (2011): "A new theory of nucleation", in Phase Transitions, A Multinational J., 84:11-12, 999-1014.
[13]   van der Put T.A.C.M. (2010): "Theoretical derivation of the WLF(= glass transition)- and annealing equations", Journal of Non-Crystalline Solids 356 (2010) 394–399 .
[14]   May Y.W., On the velocity-dependent fracture toughness of wood, Wood Science 18 (1975) 1.
[15]   Valentin G.H., Boström L., Gustafsson P.J., Ranta-Maunus A., Gowda S., RILEM state-of-the-art report on fracture mechanics, VTT Report 1262, Espoo, Finland, 1991.
[16]   van der Put T.A.C.M. (2011): A new theory of nucleation, in: Phase Transitions: A Multinational Journal, 84:11-12, 999-1014.
[17]   van der Put T.A.C.M. (2009) A continuum failure criterion applicable to wood, J Wood Sci 55:315–322.
[18]   Gopu, Vijaya K. A. (1987) Validity of Distortion-Energy-Based Strength Criterion for Timber Members, *J. Struc. Eng.* 113, No. 12 pp. 2475-2487.
[19]   van der Put T.A.C.M. (1982) A general failure criterion for wood, Proceed. 15th CIB-IUFRO Timber Eng. Group Meeting, Boras, Sweden.
[20]   Hemmer K. (1985) Versagensarten des Holzes der Weisstanne unter mehrassige Beanspruchung, Dissertation, University of Karlsruhe, Karlsruhe.
[21]   Susanti CME, Nakao N., Yoshihara H. Examination of the Mode II fracture behaviour of wood with a short crack in an asymmetric four-point bending test Eng. Fract. Mech. 2011; 78 – 16: 2775-2788
[22]   Wu E.M (1967) Application of fracture mechanics to anisotropic plates. J Appl Mech 34:967–974.
[23]   van der Put T.A.C.M. (2012) Discussion of: "Mode II fracture mechanics properties of wood measured by the asymmetric four-point bending test using a single-edge-notched specimen of H Yoshihara in Eng. Frac. Mech. 75 pp 4727-4739" in Eng. Frac. Mech. 90 pp 172-179 .
[24]   Mall S., Murphy J.F., Shottafer J.E. "Criterion for Mixed Mode Fracture in Wood" J. Eng. Mech. 109(3) 680-690, June 1983.